Available online at www.sciencedirect.com

ScienceDirect

Neuromuscular Disorders 29 (2019) 358–367

www.elsevier.com/locate/nmd

Distinct segregation of the pathogenic m.5667G>A mitochondrial tRNA^{Asn} mutation in extraocular and skeletal muscle in chronic progressive external ophthalmoplegia

Elena Schlapakow[a,d], Viktoriya Peeva[b], Gábor Zsurka[b,c], Monika Jeub[a], Bettina Wabbels[e], Cornelia Kornblum[a,d], Wolfram S. Kunz[b,c,*]

[a] *Department of Neurology, University Hospital of Bonn, Germany*
[b] *Division of Neurochemistry, Institute of Experimental Epileptology and Cognition Research, University of Bonn, Sigmund-Freud-Str. 25, D-53105 Bonn, Germany*
[c] *Department of Epileptology, University of Bonn, Germany*
[d] *Center for Rare Diseases, University Hospital of Bonn, Germany*
[e] *Department of Ophthalmology, University of Bonn, Germany*

Received 18 September 2018; received in revised form 8 January 2019; accepted 19 February 2019

Abstract

Chronic progressive external ophthalmoplegia (CPEO) is a frequent clinical manifestation of disorders caused by pathogenic mitochondrial DNA mutations. However, for diagnostic purposes skeletal muscle tissue is used, since extraocular muscle tissue is usually not available for work-up. In the present study we aimed to identify causative factors that are responsible for extraocular muscle to be primarily affected in CPEO. We performed comparative histochemical and molecular genetic analyses of extraocular muscle and skeletal muscle single fibers in a case of isolated CPEO caused by the heteroplasmic m.5667G>A mutation in the mitochondrial tRNA^{Asn} gene (*MT-TN*). Histochemical analyses revealed higher proportion of cytochrome *c* oxidase deficient fibers in extraocular muscle (41%) compared to skeletal muscle (10%). However, genetic analyses of single fibers revealed no significant difference either in the mutation loads between extraocular muscle and skeletal muscle cytochrome *c* oxidase deficient single fibers (extraocular muscle 86% ± 4.6%; skeletal muscle 87.8 % ± 5.7%, $p = 0.246$) nor in the mutation threshold (extraocular muscle 74% ± 3%; skeletal muscle 74% ± 4%). We hypothesize that higher proportion of cytochrome *c* oxidase deficient fibers in extraocular muscle compared to skeletal muscle might be due to facilitated segregation of the m.5667G>A mutation into extraocular muscle, which may explain the preferential ocular manifestation and clinically isolated CPEO.

Keywords: Chronic progressive external ophthalmoplegia (CPEO); mt-tRNA^{Asn}; Single muscle fiber; Heteroplasmy; mtDNA copy number.

1. Introduction

Chronic progressive external ophthalmoplegia (CPEO) is the most frequent mitochondrial myopathy [1], which is characterised by a slowly progressive paresis of extraocular muscles leading to ptosis and restriction of eye movements with subsequent strabism and – less frequently – diplopia. CPEO is caused by mutations either in the mitochondrial (mt) or the nuclear genome both resulting in a perturbance of mitochondrial oxidative phosphorylation. Sporadically occurring single large-scale mtDNA rearrangements (deletions or duplications) as well as sporadically or maternally inherited mtDNA point mutations are attributed to primary mtDNA mutagenesis, whereas secondary mtDNA rearrangements are caused by nuclear gene mutations leading to multiple mtDNA deletions or depletions. More than half of the mtDNA point mutations are located in genes coding for mt-tRNAs, which on their part comprise only 5–10% of the whole mitochondrial genome [2,3]. Due to the high variability of the mitochondrial genome, distinguishing pathogenic nucleotide exchanges from polymorphic variants can be challenging.

* Corresponding author at: Division of Neurochemistry, Institute of Experimental Epileptology and Cognition Research, University of Bonn, Sigmund-Freud-Str. 25, D-53105 Bonn, Germany.
E-mail address: wolfram.kunz@ukbonn.de (W.S. Kunz).

https://doi.org/10.1016/j.nmd.2019.02.009
0960-8966/

This is the second independent report of the m.5667G>A mutation, which has been previously described in a mtDNA screening of patients with suspected mitochondrial diseases without experimental confirmation of pathogenicity [4]. Here we demonstrate for the first time its definitive pathogenicity by the evidence of mutation segregation with the biochemical defect on single muscle fiber level. This analysis is a crucial component of the revised pathogenicity scoring system for mt-tRNA mutations [5] and the gold-standard investigation for assigning their pathogenicity [6].

The molecular background of the preferential affection of extraocular muscle (EOM) in CPEO is poorly understood. Until now, only one single study has systematically compared EOM and skeletal muscle (SKM) of CPEO patients with primary and secondary mtDNA defects [7]. In cases of primary mtDNA deletions the authors demonstrated a lower mutation threshold in EOM as a possible explanation of more cytochrome *c* oxidase (COX)-deficient fibers in EOM compared to SKM. By contrast, they failed to find significant differences in the absolute level of COX-deficiency in two cases of mtDNA point mutations as well as in the mutational threshold between EOM and SKM in only one investigated case of these two mutations [7].

In the present case of isolated CPEO harboring the pathogenic m.5667G>A mutation in the $tRNA^{Asn}$ gene, we have addressed possible reasons for the preferential clinical EOM involvement by use of comparative histochemical and genetic single muscle fiber analyses of EOM and SKM.

2. Materials and methods

2.1. Standard protocol approval, registration, and patient consent

This study was conducted according to the Declaration of Helsinki (2000) of the World Medical Association and the guidelines of the University Hospital of Bonn Ethical Committee. Written informed consent was obtained from the parents of the patient.

2.2. Case description

A 14-year-old boy of Turkish ethnic origin presented with a right-sided upper eye lid ptosis that developed during an acute mild febrile illness. After recovery, the ptosis persisted, and the patient complained of intermittent double vision. His further past medical history was uneventful. At first presentation, the clinical examination revealed the right-sided upper eye lid ptosis, and a bilateral asymmetric restriction of extraocular eye movements leading to divergent and vertical strabism. There were no other pathologic findings, especially no signs of hearing loss, muscle weakness, peripheral nervous system involvement, cardiac or endocrinological problems. The diagnostic work-up included a broad laboratory analysis of blood and cerebrospinal fluid (CSF), a magnetic resonance imaging (MRI) of the brain, and neurophysiological examinations including repetitive nerve stimulation studies. There were no remarkable findings, in particular creatine kinase (CK) levels in the blood and lactate levels in the CSF were within the normal range. Open skeletal muscle biopsy was performed at the age of 16 years, and histochemical and biochemical analyses showed typical signs of a mitochondrial myopathy. In the course of time the patient developed permanent double vision and underwent three corrective strabismus surgeries from the age of 17 years on.

There were no further family members affected by neurological or neuromuscular symptoms. The patient and all family members unfortunately declined further genetic analyses of blood, buccal mucosa, and urine sediment.

2.3. Muscle histology and histochemistry

M. vastus lateralis (SKM) from open skeletal muscle biopsy as well as M. rectus superior and M. rectus medialis specimens (EOM) from resection during corrective strabismus surgeries were used for further analyses. The samples were immediately frozen in isopentane cooled to liquid nitrogen temperature. Consecutive cryostat 10 μm sections of SKM were histologically and histochemically analysed including modified Gomori's trichrome, myofibrillar actomyosin adenosine triphosphatases (mATPases at pH 4.2, 4.6, 9.4) and combined succinate dehydrogenase (SDH)/cytochrome *c* oxidase (COX) histochemical reactions as described by Dubowitz [8]. Consecutive cryostat 10 μm sections of EOM were analysed by modified Gomori's trichrome and combined SDH/COX histochemical reactions.

Fiber types of SKM were distinguished based on the mATPase staining at pH 4.6. The differentiation of EOM fiber types in consecutive sections was not feasible on the basis of mATPase stainings due to the short length and the irregular orientation of single fibers.

We calculated the number of COX-deficient/SDH-positive fibers per 500 SKM fibers and per 100 EOM fibers on COX/SDH double-stained sections to determine the approximate percentage of COX-deficient/SDH-positive fibers in each muscle sample.

2.4. Biochemical investigations

Respiratory chain enzyme activities (rotenone sensitive NADH–CoQ_1 oxidoreductase [complex I], cytochrome *c* oxidase (COX) [complex IV]) and citrate synthase (CS) activity were measured spectrophotometrically in SKM homogenate by standard methods according to earlier description [9]. To minimize potential effects of fiber type variation or mitochondrial proliferation, results were corrected by normalization of data to the mitochondrial marker enzyme CS and given in units/g of wet weight.

The analysis of EOM respiratory chain enzyme activities was not feasible due to the small volume of the biopsy.

2.5. mtDNA mutation analysis

Total DNA was extracted from 30 mg skeletal muscle tissue using the QIAamp DNA Mini Kit (Qiagen, Hilden, Germany). Large mtDNA deletions were excluded by amplification of

six large overlapping fragments of the mitochondrial genome using long-range PCR. Thereafter, the whole mitochondrial genome was analysed by a sequence analysis of 30 overlapping PCR fragments performed by a commercial sequencing service (Eurofins, Ebersberg, Germany). Sequence data were compared with the revised mtDNA Cambridge reference sequence for human mtDNA (GenBank accession number NC_012920.1).

2.6. Single muscle fiber laser microdissection

We applied a laser microdissection technique (PALM MicroBeam system) to analyse m.5667G>A mutation loads in COX-deficient and COX-positive single muscle fibers. Individual skeletal muscle fibers were cut from unstained 10 μm air-dried cryostat sections mounted on membrane slides (ZEISS) that had been subjected to sequential immersion in 70% ethanol, 95% ethanol, absolute ethanol and xylen. As the unstained sections were located in between two COX/SDH stained sections, corresponding individual muscle fibers that were positive or negative for COX-staining could easily be identified. Due to the short fiber length this work-up was not possible for EOM single fiber analysis. Therefore, single extraocular muscle fibers were microdissected from air-dried 10 μm cryostat sections mounted on membrane slides (ZEISS) and COX/SDH double-stained – in deviation from the standard protocol – not longer than 15 min for each histochemical reaction. A previous analysis of microdissected single muscle fibers that derived from histochemically differently processed consecutive sections of the same muscle fiber had not shown any effect on mtDNA quality [10].

30 COX-negative and 27 COX-positive SKM single fibers and 20 COX-negative and 28 COX-positive EOM single fibers were cut and analysed.

The cut single muscle fibers from skeletal and extraocular muscle sections were catapulted into a tube cap containing 20 μl of magnesium-free PCR buffer, 10x diluted Tris-EDTA buffer, 0.5% Tween 20, and 1 mg/ml proteinase K. After a short centrifugation, incubation at 55 °C for 30 min and inactivation of the proteinase K at 95 °C for 10 min, 8 μl of each sample were subjected to mismatched primer-PCR and restriction analysis, and 10 μl of the remaining volume were subjected to single fiber real-time PCR.

2.7. Mismatched primer-PCR and restriction fragment length polymorphism

To detect the m.5667G>A point mutation, a mismatched primer was designed to introduce a restriction site at position 5670: 5′-AACTAAGTGTTTGTGGGTTTAAGGCC-3′ (nucleotides position 5693–5668 according to rCRS for human mtDNA, mismatched nucleotide underlined). This primer was used together with the forward primer 5′-CTTAATTTCTGTAACAGCTAAGGACTGC-3′ (nucleotides position 5569–5596 according to rCRS for human mtDNA) resulting in a 125 bp product that was subsequently digested with two different restriction endonucleases at 37 °C, one cutting in the presence of the mutant allele (StuI), the other in the presence of the wild-type allele (Sau96I).

Amplification condition for mismatch-PCR was as follows: initial denaturation at 95 °C for 10 min; 35 cycles of denaturation at 95 °C for 15 s, annealing at 66 °C for 30 s, and extension at 72 °C for 1 min; and finally 72 °C for 7 min.

Restriction fragments were separated by electrophoresis through 10% denaturing polyacrylamide gel (Fig. 1A), and visualised by SYBR Green I staining (Sigma-Aldrich, Steinheim, Germany). Proportions of wild-type and mutant mtDNA products were calculated from band intensities being corrected with local area background subtraction using Image J analysis software (http://rsb.info.nih.gov.ij). The relative proportions of the mutation loads were calculated from averages of two different restriction endonuclease digestions to control for the completeness of digestion.

2.8. Calculation of the mutational thresholds and the bulk muscle heteroplasmy levels

The mutation threshold for EOM and SKM was determined as average of heteroplasmy levels from fibers located in the threshold zone (switch from COX positive to COX negative) in Fig. 3C (fibers 1–5 for EOM and fibers 6–10 for SKM).

In contrast to SKM, EOM fibers are embedded in ample connective tissue (Fig. 2A and 2B). To correct for this variable amount of connective tissue, we calculated the bulk muscle heteroplasmy levels of EOM and SKM according to the following formula:

bulk muscle heteroplasmy level
= (percentage of COX-positive fiber numbers on COX/SDH sections
× mean heteroplasmy level of COX-positive single fibers)
+ (percentage of COX-negative fiber numbers on COX/SDH sections
× mean heteroplasmy level of COX-negative single fibers).

2.9. Single fiber real-time PCR

To quantify the single fiber mtDNA copy number we performed real-time PCR of single fiber lysates using the BIO-RAD C1000 Touch Thermal Cycler CFX 96™ Real-Time System. The mitochondrial primers 3922F (5′-GAACTAGTCTCAGGCTTCAACATCG-3′) and 4036R (5′-CTAGGAAGATTGTAGTGGTGAGGGTG-3′) were chosen for specific amplification of a short fragment in the *MT-ND1* gene. A total volume of 25 μl reaction mixture was composed of 10 μl of single fiber DNA lysate, 2.5 μl nanopure water, 11.9 μl 2x SYBR Green qPCR Master Mix (Bimake, U.S.A.) and 0.3 μl of each primer (12.5 pmol/μl). The initial denaturation step was at 95 °C for 7 min followed by 45 cycles including a denaturation step at 95 °C for 15 s and a combined annealing and elongation step at 62.5 °C for 30 s. Melting curve analysis was used to validate the PCR products. A non-template control (H_2O) as well as a fibroblast control (from a control subject) was included in each experiment.

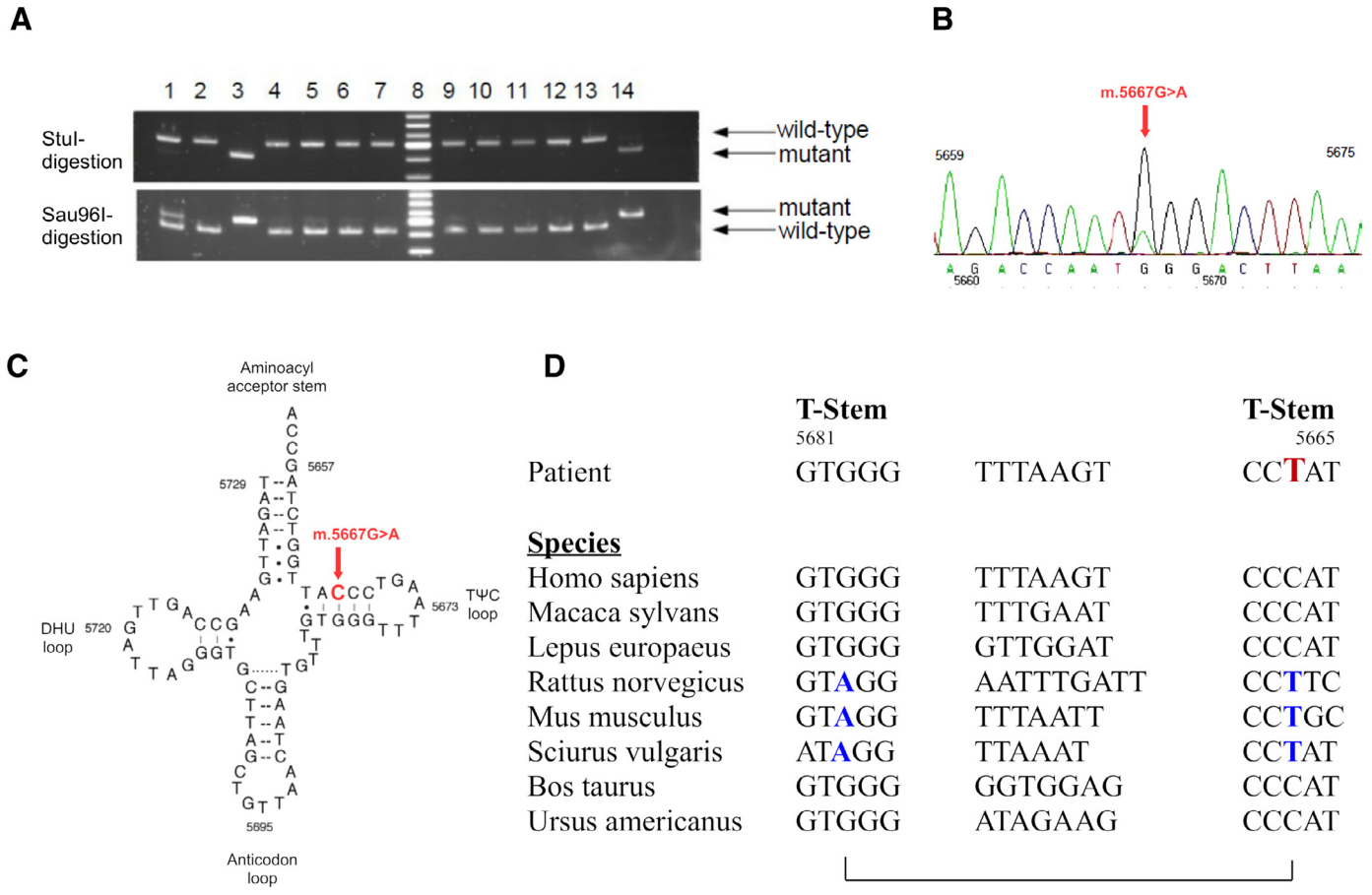

Fig. 1. Heteroplasmic pathogenic m.5667G>A mutation in the mitochondrial $tRNA^{Asn}$. (A) Restriction fragment length polymorphism analysis with two different restriction endonuclease digestions, one cutting in the presence of the mutant allele (StuI), the other in the presence of the wild-type allele (Sau96I): lane 1: patient's bulk SKM; lane 2: mtDNA from a healthy subject's blood sample as an internal control for wild-type allele; lane 3: synthetic control template DNA for mutant allele; lanes 4–7 as lanes 9–13: SKM single muscle fibers that were positive for COX-staining with dominating wild-type mtDNA; lane 14: SKM single muscle fiber that was negative for COX-staining with dominating mutant mtDNA; lane 8: molecular weight marker. (B) Sanger sequence electropherogram showing the heteroplasmic m.5667G>A point mutation in patient's skeletal muscle mtDNA. (C) Position of the m.5667G>A mutation in the predicted two dimensional mt-$tRNA^{Asn}$ structure (modified according to Mamit-tRNA, http://mamit-trna.u-strasbg.fr/). (D) Interspecies alignment of the TΨC-stem and -loop in the mt-$tRNA^{Asn}$ demonstrating the high phylogenetic conservation of the Watson-Crick base pairing between the affected nucleotide with the opposite nucleotide in the TΨC-stem. The position of the m.5667G>A mutation itself is not strictly conserved in mammals. However, in the case of its substitution in some species, the high conservation of the Watson-Crick base pair is maintained by an altered nucleotide in the opposite side of the TΨC-stem (shown in blue).

For relative quantification data points were fitted with a 4-parameter Chapman curve $[y = y_0 + a(1 - e^{-bx})^c]$ using SigmaPlot, and C_t values were defined as x parameters of inflection points of the sigmoid curves $[C_t = \ln(c) / b]$ [11]. To determine the relative amounts of mtDNA copy number per single muscle fiber we used the $2^{-\Delta Ct}$ method [12] applying the lowest C_t value of all measured single fiber lysates ($C_{t\ min}$) as the reference value and normalized to fiber areas in μm^2 (A_i) according to the formula $2^{-[Ct\ i - Ct\ min]} / A_i$. Fiber areas were determined using the dissection microscope software (PALM MicroBeam).

2.10. Statistical analysis

Group comparisons with preceding variance analyses were performed applying two-tailed unpaired Student's t-test (Prism version 3 statistical software; GraphPad Prism, San Diego, CA). All results are expressed as mean ± SD.

3. Results

3.1. Mosaic respiratory chain enzyme deficiency in a patient with CPEO

Histochemical analysis of the SKM specimens showed a typical mosaic pattern in the combined COX/SDH histochemical reaction with on average 10% COX-deficient/SDH-positive fibers. The presence of ragged-red fibers in the modified Gomori's trichrome staining indicated compensatory mitochondrial proliferation (Fig. 2A).

Histochemical analysis of the EOM revealed with 41% a higher percentage of COX-deficient/SDH-positive fibers in comparison with the SKM (Fig. 2B). The modified Gomori's trichrome staining showed numerous ragged-red-fibers in EOM.

Mitochondrial respiratory chain enzyme activities were spectrophotometrically measured in the SKM homogenate.

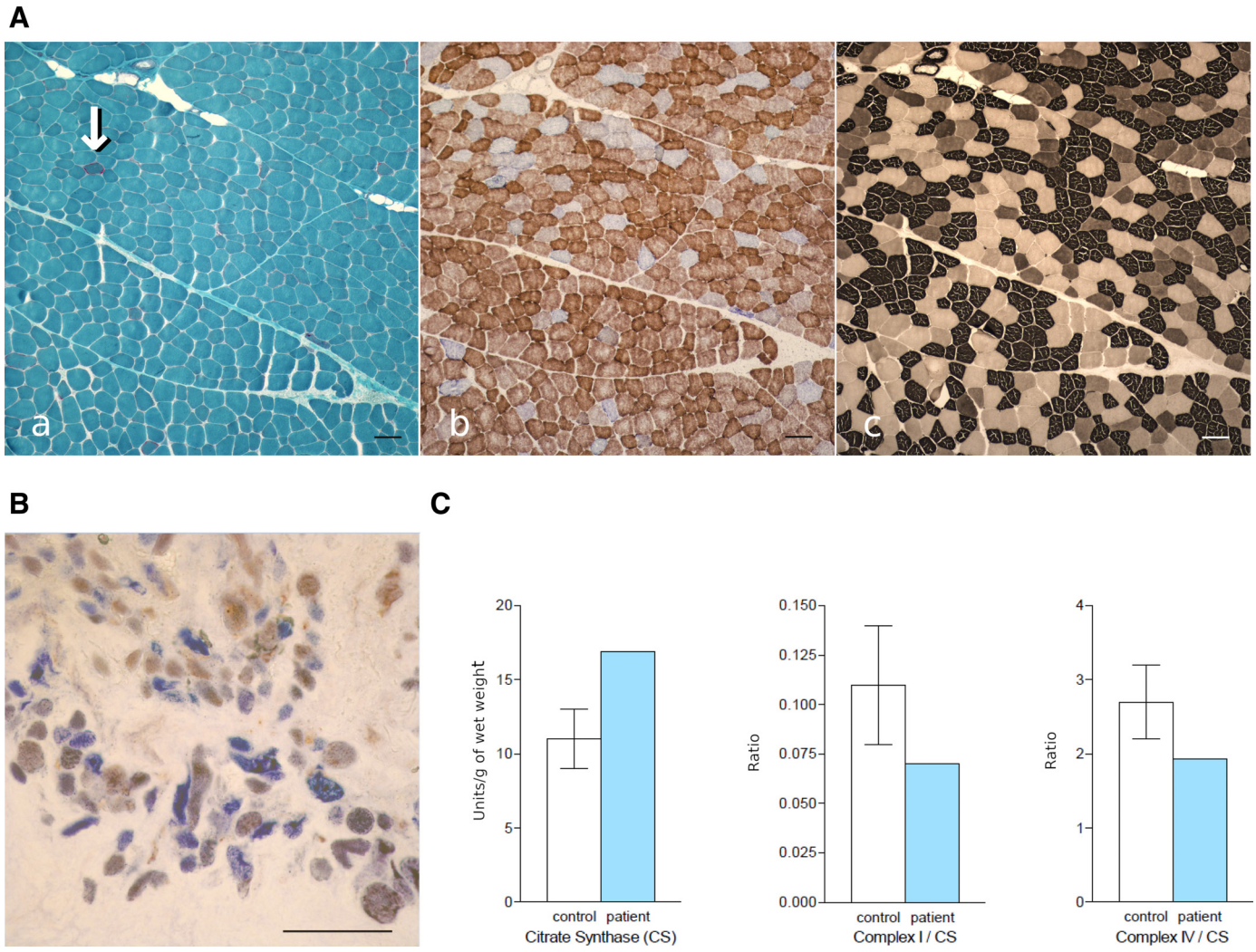

Fig. 2. Respiratory chain enzyme deficiency in muscle tissues. (A) Skeletal muscle (M. vastus lateralis): (a) modified Gomori's trichrome staining with ragged-red fiber (arrow), (b) combined COX/SDH staining, (c) mATPase staining at pH 4.6. Scale bars: 100 μm. (B) Extraocular muscle (M. rectus medialis), combined COX/SDH staining. Scale bar: 100 μm. (C) Complex I and IV activities and citrate synthase (CS) activity spectrophotometrically measured in skeletal muscle homogenate. To minimize potential effects of fiber type variation or mitochondrial proliferation, complex I and IV activities were normalized to CS. Open bars with mean ± SD of 200 controls.

While absolute activities of respiratory chain complexes I and IV displayed results within the reference values, the activities of complex I and IV normalized to CS showed decreased relative activity levels, thus indicating a combined respiratory chain deficiency. The activity of the mitochondrial matrix marker enzyme CS was elevated compared to reference values as a sign of higher mitochondrial content, most probably due to compensatory mitochondrial proliferation [13] (Fig. 2C).

3.2. Heteroplasmic pathogenic mutation in the MT-TN gene and homoplasmic polymorphic variant m.7082C>A in the MT-COI gene

After large scale deletions have been excluded by long-range PCR, direct sequence analysis of the whole mitochondrial genome of the SKM was performed. The comparison of the sequence data with the revised Cambridge reference sequence for human mtDNA (GenBank accession number NC_012920.1) showed already known homoplasmic non-pathogenic polymorphisms, the combination of which is typical for the mitochondrial haplogroup K1a8. Furthermore, the well-known m.185G>A sequence variation, also considered as polymorphism, within the hypervariable segment 2 (*MT-HV2*) in the non-coding mtDNA control region in the D-loop [14] was detected in a heteroplasmic state. Additionally, two point mutations that are not listed in the human mtDNA databases (MITOMAP, http://www.mitomap.org; Human Mitochondrial Genome Database, http://www.genpat.uu.se/mtDB) were found: a heteroplasmic G>A transition at position 5667 in the *MT-TN* gene [accession number SCV000803665, available at ClinVar - NCBI – NIH, https://www.ncbi.nlm.nih.gov/clinvar/] (Fig. 1B), and a homoplasmic C>A transversion at position 7082 in the *MT-CO1* gene [accession number SCV000803740, available at ClinVar - NCBI – NIH,

https://www.ncbi.nlm.nih.gov/clinvar/]. The assessment whether a novel point mutation is pathogenic or just a polymorphic variant can be challenging, especially when presenting in a homoplasmic condition. The previously undescribed homoplasmic m.7082C>A mutation within the *MT-CO1* gene, that codes for subunit COI of the respiratory chain complex IV (cytochrome *c* oxidase), changes codon 393 from TTC to TTA which corresponds to an amino acid change of phenylalanine to leucine (Phe393Leu). Noteworthy, the search for already known polymorphic sites of nucleotides in the human mtDNA database MITOMAP (http://www.mitomap.org) revealed in 45,494 sequences the occurrence of 43 nonsynonymous substitutions at position m.7080T>C, the first nucleotide of the same codon 393, that equally lead to the amino acid change from phenylalanine to leucine. Thus, the homoplasmic m.7082C>A transversion is rather a neutral polymorphism without any pathogenic contribution than a deleterious mutation. Furthermore, a deleterious homoplasmic mutation in the *MT-CO1* gene would be expected to cause an uniform isolated complex IV deficiency in all fibers, which was not observed in the present case.

Analyses of the heteroplasmic m.5667G>A mutation revealed 48% m.5667G>A mutation loads in extraocular bulk muscle tissue and 19% in skeletal bulk muscle tissue. The position m.5667 itself is not strictly conserved in mammals, but the Watson-Crick base pairing with the corresponding nucleotide at the opposite side of the TΨC-stem is strictly maintained in all known sequences (Fig. 1D). This is suggestive of the high importance of position m.5667 for the structure and functionality of mt-tRNA^{Asn}.

To further evaluate the potentially pathogenic role of the m.5667G>A mutation and to analyse mutational thresholds in SKM and EOM, mutation loads in mtDNA samples isolated from single fibers of SKM and EOM were determined and compared. The COX-negative SKM fibers (87.8% ± 5.7%, $n = 30$) and COX-negative EOM fibers (86.0% ± 4.6%, $n = 20$) harbored significantly higher mutational loads ($p < 0.0001$ for SKM and $p < 0.0001$ for EOM) than COX-positive SKM fibers (11.0% ± 13%, $n = 27$) and COX-positive EOM fibers (27.1% ± 27.2%, $n = 28$). This confirms the causative role of the m.5667G>A mutation for the biochemical defect on the single cell level in both tissues. There was neither a significant difference in mutational loads of COX-negative fibers between SKM and EOM ($p = 0.2460$) nor a significant difference in the mutational threshold (SKM 74% ± 4%; EOM 74% ± 3%). Thus, the isolated ocular phenotype cannot be explained by a lower threshold of the mutation in EOM compared to SKM. Interestingly, there was a significantly lower mutational load in COX-positive SKM fibers (11.0% ± 13.0%, $n = 27$) compared to COX-positive EOM fibers (27.1% ± 27.2%, $n = 28$; $p = 0.0072$) (Fig. 3A).

Remarkably, some EOM as well as SKM single fibers that were located in the threshold range and had comparable mutation loads showed highly variable COX activities (Fig. 3A).

3.3. mtDNA copy numbers in single fibers

We detected significant mtDNA proliferation in single muscle fibers with compromised oxidative phosphorylation of both muscle types, EOM and SKM: The mean copy number of total mtDNA in COX-deficient EOM fibers (149.4 copies/μm^2 ± 168.5 copies/μm^2; $n = 20$) was 2.3-fold higher compared to COX-positive EOM fibers (65.8 copies/μm^2 ± 66.7 copies/μm^2, $n = 28$, $p = 0.0212$). Also the mean copy number of total mtDNA in COX-deficient SKM fibers (85.2 copies/μm^2 ± 73.9 copies/μm^2; $n = 30$) was 2.2-fold higher compared to COX-positive SKM fibers (38.5 copies/μm^2 ± 21.7 copies/μm^2, $n = 27$, $p = 0.0026$).

We observed a higher total mtDNA copy number in COX-deficient as well as in COX-positive EOM single fibers compared to SKM single fibers. Although the difference between the mean total mtDNA copy number in COX-deficient EOM fibers (149.4 copies/μm^2 ± 168.5 copies/μm^2; $n = 20$) compared to the mean total mtDNA copy number in COX-deficient SKM fibers (85.2 copies/μm^2 ± 73.9 copies/μm^2; $n = 30$, $p = 0.0709$) did not reach statistical significance, the higher mtDNA copy number of COX-deficient EOM fibers is reflected in the stronger histochemical reaction for SDH activity (dark blue in Fig. 2B) compared to SKM COX-deficient fibers (pale blue in Fig. 2A (b)). A statistical significant higher mean total mtDNA copy number was observed in COX-positive EOM fibers (65.8 copies/μm^2 ± 66.7 copies/μm^2, $n = 28$) than in COX-positive SKM fibers (38.5 copies/μm^2 ± 21.7 copies/μm^2, $n = 27$, $p = 0.0482$). These findings corroborate higher absolute numbers of mitochondrial DNA in EOM fibers compared to SKM fibers (Fig. 3B).

We detected a number of fibers that, despite of harboring comparable mutation loads, displayed different COX activities. We hypothesized that increased mtDNA copy numbers imply higher amounts of the wild-type mtDNA which could result in preserved functional respiration. However, the determined mtDNA copy numbers did not correlate with COX-positivity in single muscle fibers with heteroplasmy degrees close to the threshold value. (Fig. 3C).

3.4. SKM single muscle fiber types

In general, type I skeletal muscle fibers (oxidative fibers) have a higher mitochondrial content than type II muscle fibers (glycolytic fibers) [1]. To exclude a fiber type biased data presentation, the fiber type of each individual microdissected and analysed single SKM fiber has been identified on the consecutive mATPase stained section (at pH 4.6). The distribution of fiber types was comparable in the analysed COX-positive and COX-negative SKM single fibers (Table 1). For technical reasons a comparable assignment of fiber types to EOM single muscle fibers was not possible due to their short length and irregular orientation in the consecutive sections.

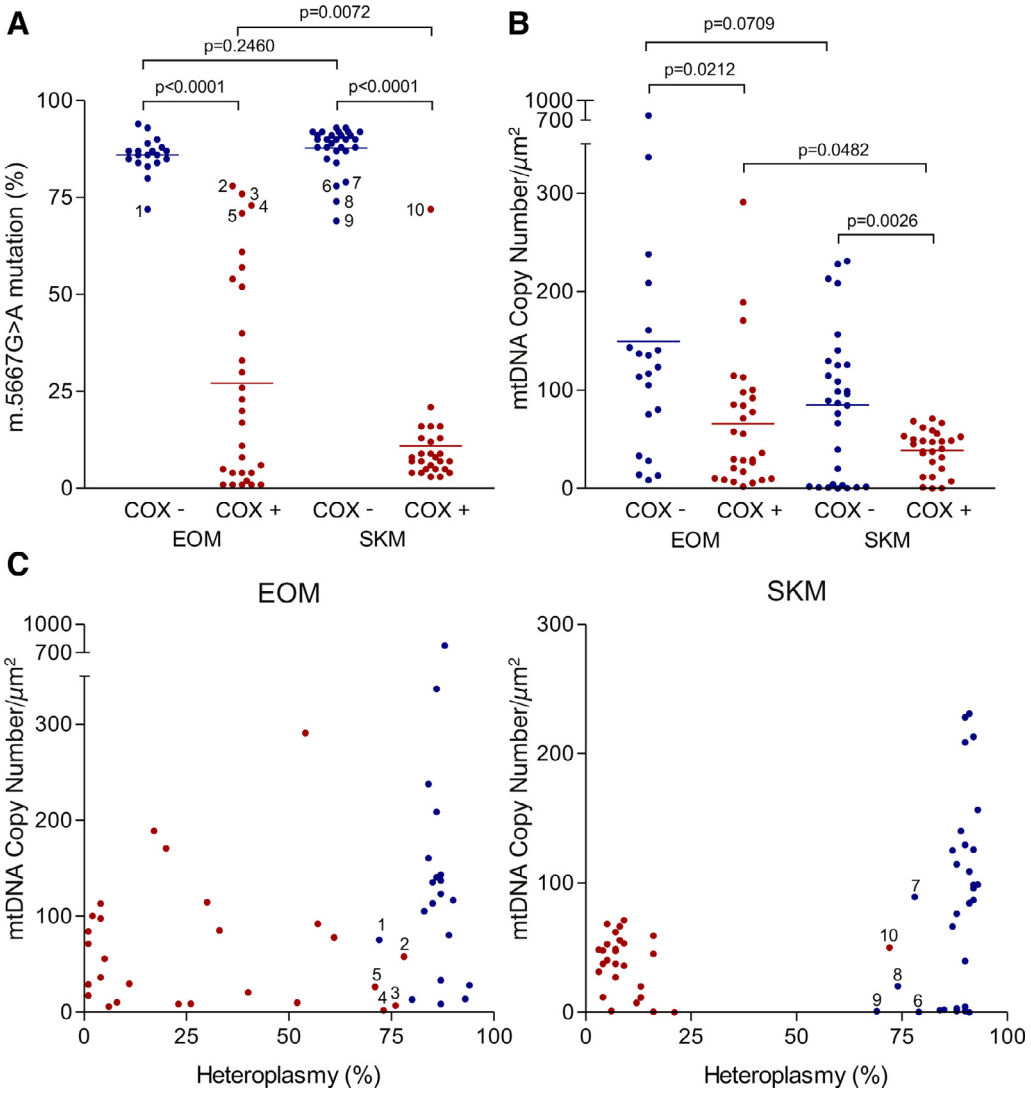

Fig. 3. Mitochondrial genotypes of single muscle fibers. (A) m.5667G>A mutation loads in single muscle fibers of EOM (COX-negative $n=20$, COX-positive $n=28$) and SKM (COX-negative $n=30$, COX-positive $n=27$). Selected single muscle fibers with similar mutation loads but distinct COX activity are indicated with numbers 1 to 10. (B) mtDNA copy number/μm^2 in 10 μm-thick single muscle fiber sections from EOM (COX-negative $n=20$, COX-positive $n=28$) and SKM (COX-negative $n=30$, COX-positive $n=27$). (C) Relation between copy number and heteroplasmy level of single muscle fibers of EOM (COX-negative n=20, COX-positive $n=28$) and SKM (COX-negative $n=30$, COX-positive $n=27$). Blue=COX-negative fibers; Red=COX-positive fibers. In A and B, horizontal lines indicate the mean value. In B and C, the copy numbers were multiplied by the factor 10^6 for graphical illustration.

Table 1
Muscle fiber types of analysed SKM single muscle fibers, based on mATPase staining (pH 4.6). FT=fiber type; n.i.=not identifiable.

	COX-negative						COX-positive			
	FT1	FT2a	FT2b	FT2c	n.i.		FT1	FT2a	FT2b	FT2c
Σ=30	11	14	1	1	3	**Σ=27**	11	13	2	1
%	37%	47%	3%	3%	10%	*%*	41%	48%	7%	4%

4. Discussion

In the present study, first we proved the pathogenicity of the m.5667G>A mutation by demonstrating its segregation with the biochemical defect in single muscle fibers and second we specifically addressed potential reasons for the selective clinical manifestation of CPEO in the present case of m.5667G>A mutation by comparative histochemical and profound molecular genetic analyses of EOM and SKM samples.

Being not registered in the human mtDNA databases (MITOMAP, http://www.mitomap.org; Human Mitochondrian Genome Database, http://www.genpat.uu.se/mtDB) and therefore absent in 45,494 featuring full length human mitochondrial GenBank sequences, the m.5667G>A mutation was first regarded as a „novel“ mutation. However, meticulous literature research revealed a yet existing description of the m.5667G>A mutation in a cohort study in which mtDNA screening of patients with a suspected mitochondrial disease had been performed [4], however differently from the present

Table 2
Described mutations in the *MT-TN* gene (nucleotide position m.5657 – m.5729).

Mutation	tRNA-position	Haplotype	Gender / Age at onset, (age at the time of diagnosis)	Clinical manifestation	Histology	Respiratory chain activities in muscle tissue	Level of heteroplasmy in different tissues	Mutation load in COX-negative single muscle fibers	Reference
5658C>T	Acceptor stem	H_3	♂ / 39	CPEO, M	RRF, COX-	↓CI, ↓CIII, ↓CIV	SKM 65%, U 17%, B 4%	SKM > 94%	[15]
5667G>A	TΨC stem	K1a	♂ / 14	CPEO	RRF, COX-	↓CI, ↓CIV	SKM 19%, EOM 41%	SKM 87.8%, EOM 86%	present report
5667G>A	TΨC stem	H	♂ / < 16	Ptosis	RRF, COX-	normal	n.d.	n.d.	[4]
5669G>A	TΨC stem	n.d.	♂ / 10 (11)	EI	RRF, COX-	↓CI, ↓CIII, ↓CIV	SKM 75%, FB 0%, B 0%	n.d.	[16]
5690A>G	Anticodon stem	H7	♀ / 13	CPEO, M	RRF, COX-	n.d.	SKM 35%, B 0%, U 0%	SKM 86.8 ± 18,3%	[17]
5692A>G	Anticodon loop	n.d.	not reported	CPEO, M, N, A, H	RRF	↓CI, ↓CIV	SKM 56%	n.d.	[18] [19]
5692T>C	Anticodon loop	n.d.	♂ / 56	CPEO, M, EI, E, A, H, N	RRF, COX-	↓CIV	SKM 46%, FB 0%, B 0%	SKM 88.2%	[20]
5693A>G	Anticodon loop	n.d.	♂ / 2 month	lethal MOF	COX-	↓↓CI, ↓↓CIV	Homoplasmic SKM 99%, B 99%	SKM ~ 99%	[21]
5698G>A	Anticodon loop	H	♀ / 33	CPEO	COX-	normal	n.d.	n.d.	[20]
5698G>A	Anticodon loop	n.d.	♂ / 56	M, EI, CPEO	RRF, COX-	normal	SKM 80%, B 20%	SKM 77.1 ± 6.0%	[22]
5703C>T	Anticodon stem	n.d.	♀ / 27	CPEO, F	RRF, COX-	↓CI, ↓CIII, ↓CIV, ↓CV	SKM 69%, FB 6%, B 4%	SKM 97–100%	[23]
5703C>T	Anticodon stem	n.d.	not reported	CPEO, F, ETA	n.d.	n.d.	n.d.	n.d.	[24]
5703G>A	Anticodon stem	n.d.	♀ / 4 (16)	CPEO, F, ETA	RRF, COX-	n.d.	SKM 80%, B 48%	n.d.	[25]
5709T>C	D-loop	n.d.	♀ / 29 (49)	CPEO, M, RI	RRF, COX-	n.d.	SKM 89,0%, B 21,7%	SKM 91.9 ± 1.5%	[26]
5728A>G	Acceptor stem	n.d.	♂ / 13	MOF	n.d.	↓CI, ↓CIV	SKM 97–100%, FB 50%, B 50%	> 75% (in trans-mitochondrial cybrids)	[27]
5728T>C	Acceptor stem	H	♂ / < 16	M, ptosis	RRF, COX-, Lipidosis	normal	n.d.	n.d.	[4]

↑ = elevated, ↓ = decreased, ♀ = female, ♂ = male, n.d. = not determined; A = ataxia, E = encephalopathy, EI = exercise intolerance, ETA = extremely. thin appearance, F = fatigue/ fatiguability, H = heart involvement, M = Myopathy, MOF = multiorgan failure, N = neuropathy, RI = respiratory. impairment; RRF = ragged-red fibers, COX- = cytochrome *c* oxidase deficient fibers; CI, CIII, CIV, CV = Respiratory chain complexes I, III, IV, V;. EOM = extraocular muscle, SKM = skeletal muscle, B = blood, FB = fibroblasts, U = urine.

study, without experimental confirmation of its pathogenicity. Interestingly, whereas hitherto described mutations within the $tRNA^{Asn}$ gene presented a broad spectrum of clinical manifestations from mild CPEO to multiorgan failure with exitus letalis [4, 15–27], the now twice reported m.5667G>A mutations [4] in two unrelated individuals show a remarkable similarity of the clinical phenotype with isolated CPEO of early onset (< 16 years) (Table 2). Noteworthy, there is a difference regarding the mitochondrial haplotype. Whereas in the present case the combination of the mtDNA polymorphisms indicated a K1a8 haplotype, the formerly reported m.5667G>A mutation was found in a patient carrying the H haplotype which shows that the m.5667G>A mutation is not restricted to a specific mtDNA haplotype. Thus, the occurrence of m.5667G>A in diverse mtDNA haplotypes is an additional hint to its pathogenicity and underpins its clinical relevance [20]. More than one independent report of mutation segregation with the disease phenotype in unrelated individuals is one of the criteria of the revised weighted scoring system for assigning pathogenicity to mitochondrial tRNA mutations [5,6].

Application of this revised pathogenicity scoring system confirmed the m.5667G>A mutation to be 'definitely pathogenic' as all further required critical indicators of pathogenicity have been fulfilled including: (i) the clear evidence of mutation segregation with biochemical loss of cytochrome *c* oxidase activity in single fiber studies which is considered as the gold standard for assigning pathogenicity;

(ii) the evidence of the high phylogenetic conservation of the Watson-Crick base pairing of the affected nucleotide with its opposite nucleotide in the TΨC-stem of the mitochondrial $tRNA^{Asn}$ (Fig. 1C,1D); (iii) the evidence of heteroplasmy by Sanger sequencing in bulk muscle and by restriction fragment length polymorphism analysis in single muscle fibers; (iv) the evidence of impaired oxidative phosphorylation by the typical mosaic pattern of COX activity loss in histochemical tissue analyses, and by decreased respiratory chain complex I and IV activities when normalized to citrate synthase activity in biochemical tissue analyses.

To investigate potential reasons for the selective clinical impairment of EOM in the present case of isolated CPEO we performed comparative histochemical and profound molecular genetic analyses of EOM and SKM. The higher proportion of COX-deficient fibers in EOM accompanied with higher bulk m.5667G>A mutation load in EOM compared to SKM (48% for EOM and 19% for SKM, for calculation see methods) but absent differences in mutation threshold levels between EOM and SKM is indicative of preferential segregation of the mutation to EOM. The lacking difference in mutational threshold levels between EOM and SKM underpins the hypothesis of increased mutation load in EOM as the main reason for the preferential EOM phenotype.

These findings are suggestive for a distinct m.5667G>A mutation segregation into the EOM compared to SKM and offer a possible explanation for the preferential involvement of EOM and the clinical manifestation of isolated CPEO. Such an unequal segregation of mutated and wild-type mtDNA molecules into EOM and SKM might happen at the time of the early embryological development as EOM and SKM originate from distinct precursor cell lines. EOM derives from the unsegmented paraxial head mesoderm and from the prechordal head mesoderm, whereas SKM arises from the somitic and lateral plate mesoderm [28,29]. Further consequences of the different patterns of the embryological EOM and SKM development are fundamental differences in their fiber type composition, myosin heavy chain expression and basic organization of their motor units, as described previously [30].

In comparison to SKM, EOM are discussed to be highly dependent on oxidative phosphorylation due to their highly demanding physiological properties, such as high fatigue resistance and sustained muscular contractions [30]. As a consequence, EOM are thought to be selectively vulnerable to respiratory chain dysfunction [7,31]. Some authors argue that, in cases of mitochondrial disorders but also in normal aging, the selective vulnerability to respiratory chain dysfunction might be the reason for the preferential affection of EOM [30] compared to SKM. Thus, this might be an additional cause for the clinical predominant EOM involvement in the present case of isolated CPEO.

In accordance to the "maintenance of wild-type" hypothesis, in cases of insufficient oxidative phosphorylation the entire mtDNA content is proliferated non-selectively to restore the wild-type mtDNA to its optimal level [10] as a compensatory mechanism. Consistently and in agreement with previous studies [7,30], our findings revealed significant higher mtDNA contents in EOM and SKM muscle fibers with compromised oxidative phosphorylation, probably reflecting mtDNA proliferation (Fig. 3B). Intriguingly, we did not observe a compensatory increase of mtDNA copy numbers in single muscle fibers with retained COX activity and equal high mutation loads as several COX-deficient fibers (Fig. 3C). On the contrary, COX-deficient single fibers of both EOM and SKM showed a wide range of mtDNA copy numbers including considerably higher mtDNA levels in comparison to COX-positive fibers that had rather low mtDNA copy numbers. Interestingly, high mtDNA copy numbers that were measured exclusively in COX-negative fibers with a high heteroplasmy level were not able to rescue COX activity. Thus, according to our results there is no clear correlation between the level of mtDNA copy number and COX activity. This issue could potentially be addressed by more elaborated assessment of relationship of complex IV (COX) protein abundance and mitochondrial mass in individual fibers using quantitative fluorescent immunohistochemical techniques [32].

In conclusion, we demonstrate that segregation of the heteroplasmic pathogenic m.5667G>A mutation is different in EOM and SKM, which might explain higher mutation loads and primary disease manifestation in EOM. Whether the segregation pattern described here is typical for most CPEO cases caused by mtDNA point mutations, can be only addressed by studying more EOM/SKM tissue pairs. The underlying mechanisms that lead to different segregation of mtDNA sequence variants in different tissues remain unclear and require further investigations.

Acknowledgements

The authors thank the patient for participating in this study. We are much indebted to Karin Kappes-Horn (Department of Neurology, University Hospital of Bonn) for the excellent technical assistance, Prof. F. Hochholdinger and Dr. Peng Yu (Institut für Nutzpflanzenwissenschaften und Ressourcenschutz (INRES), University Bonn, Germany) for the great assistance and help during the work with the Zeiss Microscope PALM MicroBeam.

Funding

This research was supported by grants of Deutsche Forschungsgemeinschaft (KU 911/21–2 to W.S.K. and ZS 99/3–2 to G.Z.) and BONFOR to V.P.

References

[1] Zierz S. Muskelerkrankungen. 4th ed. Stuttgart: Georg Thieme Verlag KG; 2014. p. 274.
[2] Schon EA, DiMauro S, Hirano M. Human mitochondrial DNA: roles of inherited and somatic mutations. Nat Rev Genet 2012;13(12):878–90. doi:10.1038/nrg3275.
[3] Yarham JW, Elson JL, Blakely EL, McFarland R, Taylor RW. Mitochondrial tRNA mutations and disease. Wiley Interdiscip Rev RNA 2010;1(2):304–24. doi:10.1002/wrna.27.

[4] Bannwarth S, Procaccio V, Lebre AS, Jardel C, Chaussenot A, Hoarau C, et al. Prevalence of rare mitochondrial DNA mutations in mitochondrial disorders. J Med Genet 2013;50(10):704–14. doi:10.1136/jmedgenet-2013-101604.

[5] Yarham JW, Al-Dosary M, Blakely EL, Alston CL, Taylor RW, Elson JL, et al. A comparative analysis approach to determining the pathogenicity of mitochondrial tRNA mutations. Hum Mutat 2011;32(11):1319–25. doi:10.1002/humu.21575.

[6] DiMauro S, Schon EA. Mitochondrial DNA mutations in human disease. Am J Med Genet Spring 2001;106(1):18–26. doi:10.1002/ajmg.1392.

[7] Greaves LC, Yu-Wai-Man P, Blakely EL, Krishnan KJ, Beadle NE, Kerin J, et al. Mitochondrial DNA defects and selective extraocular muscle involvement in CPEO. Invest Ophthalmol Vis Sci 2010;51(7):3340–6. doi:10.1167/iovs.09-4659.

[8] Dubowitz V, Sewry C, Oldfors A. Muscle biopsy, a practical approach. 4th ed. Oxford, UK: Saunders/Elsevier Ltd.; 2013.

[9] Wiedemann FR, Vielhaber S, Schröder R, Elger CE, Kunz WS. Evaluation of methods for the determination of mitochondrial respiratory chain enzyme activities in human skeletal muscle samples. Anal Biochem 2000;279(1):55–60. doi:10.1006/abio.1999.4434.

[10] Durham SE, Samuels DC, Cree LM, Chinnery PF. Normal levels of wild-type mitochondrial DNA maintain cytochrome c oxidase activity for two pathogenic mitochondrial DNA mutations but not for m.3243A>G. Am J Hum Genet 2007;81(1):189–95. doi:10.1086/518901.

[11] Zsurka G, Baron M, Stewart JD, Kornblum C, Bös M, Sassen R, et al. Clonally expanded mitochondrial DNA mutations in epileptic individuals with mutated DNA polymerase gamma. J Neuropathol Exp Neurol 2008;67(9):857–66. doi:10.1097/NEN.0b013e3181839b2d.

[12] Krishnan KJ, Bender A, Taylor RW, Turnbull DM. A multiplex real-time PCR method to detect and quantify mitochondrial DNA deletions in individual cells. Anal Biochem 2007;370(1):127–9. https://doi.org/10.1016/j.ab.2007.06.024.

[13] Larsen S, Nielsen J, Hansen CN, Nielsen LB, Wibrand F, Stride N, et al. Biomarkers of mitochondrial content in skeletal muscle of healthy young human subjects. J Physiol 2012;590(14):3349–60. doi:10.1113/jphysiol.2012.230185.

[14] Zsurka G, Schröder R, Kornblum C, Rudolph J, Wiesner RJ, Elger CE, et al. Tissue dependent co-segregation of the novel pathogenic G12276A mitochondrial tRNALeu(CUN) mutation with the A185G D-loop polymorphism. J Med Genet 2004;41(12):e124. doi:10.1136/jmg.2004.022566.

[15] Pinós T, Melià MJ, Ortiz N, Martinez-Vea A, Raventós-Estellé A, Gallardo E, et al. Identification of the novel mutation m.5658T>C in the mitochondrial tRNA(Asn) gene in a patient with myopathy, bilateral ptosis and ophthalmoparesis. Neuromuscul Disord 2013;23(4):330–6. doi:10.1016/j.nmd.2013.01.001.

[16] Bruno C, Cassandrini D, Fattori F, Pedemonte M, Fiorillo C, Brigati G, et al. Mitochondrial myopathy in a child with a muscle-restricted mutation in the mitochondrial transfer RNA^{Asn} gene. Biochem Biophys Res Commun 2011;412(4):518–21. doi:10.1016/j.bbrc.2011.06.155.

[17] Blakely EL, Yarham JW, Alston CL, Craig K, Poulton J, Brierley C, et al. Pathogenic mitochondrial tRNA point mutations: nine novel mutations affirm their importance as a cause of mitochondrial disease. Hum Mutat 2013;34(9):1260–8. doi:10.1002/humu.22358.

[18] Münscher C, Müller-Höcker J, Kadenbach B. Human aging is associated with various point mutations in tRNA genes of mitochondrial DNA. Biol Chem Hoppe Seyler 1993;374(12):1099–104.

[19] Seibel P, Lauber J, Klopstock T, Marsac C, Kadenbach B, Reichmann H. Chronic progressive external ophthalmoplegia is associated with a novel mutation in the mitochondrial tRNA(Asn) gene. Biochem Biophys Res Commun 1994;204(2):482–9. doi:10.1006/bbrc.1994.2485.

[20] Sternberg D, Chatzoglou E, Laforêt P, Fayet G, Jardel C, Blondy P, et al. Mitochondrial DNA transfer RNA gene sequence variations in patients with mitochondrial disorders. Brain 2001;124(Pt 5):984–94.

[21] Coulbault L, Herlicoviez D, Chapon F, Read MH, Penniello MJ, Reynier P, et al. A novel mutation in the mitochondrial tRNA ^{Asn} gene associated with a lethal disease. Biochem Biophys Res Commun 2005;329(3):1152–4. doi:10.1016/j.bbrc.2005.02.083.

[22] Spinazzola A, Carrara F, Mora M, Zeviani M. Mitochondrial myopathy and ophthalmoplegia in a sporadic patient with the 5698G>A mitochondrial DNA mutation. Neuromuscul Disord 2004;14(12):815–17. doi:10.1016/j.nmd.2004.09.002.

[23] Moraes CT, Ciacci F, Bonilla E, Jansen C, Hirano M, Rao N, et al. Two novel pathogenic mitochondrial DNA mutations affecting organelle number and protein synthesis. Is the tRNA(Leu(UUR)) gene an etiologic hot spot? J Clin Invest 1993;92(6):2906–15. doi:10.1172/JCI116913.

[24] Hao H, Moraes CT. A disease-associated G5703A mutation in human mitochondrial DNA causes a conformational change and a marked decrease in steady-state levels of mitochondrial tRNA(Asn). Mol Cell Biol 1997;17(12):6831–7. doi:10.1128/MCB.17.12.6831.

[25] Vives-Bauza C, Del Toro M, Solano A, Montoya J, Andreu AL, Roig M. Genotype-phenotype correlation in the 5703G>A mutation in the tRNA(ASN) gene of mitochondrial DNA. J Inherit Metab Dis 2003;26(5):507–8.

[26] Ronchi D, Sciacco M, Bordoni A, Raimondi M, Ripolone M, Fassone E, et al. The novel mitochondrial tRNA^{Asn} gene mutation m.5709T>C produces ophthalmoparesis and respiratory impairment. Eur J Hum Genet 2012;20(3):357–60. doi:10.1038/ejhg.2011.238.

[27] Meulemans A, Seneca S, Lagae L, Lissens W, De Paepe B, Smet J, et al. A novel mitochondrial transfer RNA(Asn) mutation causing multiorgan failure. Arch Neurol 2006;63(8):1194–8. doi:10.1001/archneur.63.8.1194.

[28] Porter JD, Baker RS, Ragusa RJ, Brueckner JK. Extraocular muscles: basic and clinical aspects of structure and function. Surv Ophthalmol 1995;39(6):451–84. doi:10.1016/S0039-6257(05)80055-4.

[29] Bohnsack BL, Gallina D, Thompson H, Kasprick DS, Lucarelli MJ, Dootz G, et al. Development of extraocular muscles requires early signals from periocular neural crest and the developing eye. Arch Ophthalmol 2011;129(8):1030–41. doi:10.1001/archophthalmol.2011.75.

[30] Yu-Wai-Man P, Lai-Cheong J, Borthwick GM, He L, Taylor GA, Greaves LC, et al. Somatic mitochondrial DNA deletions accumulate to high levels in aging human extraocular muscles. Invest Ophthalmol Vis Sci 2010;51(7):3347–53. doi:10.1167/iovs.09-4660.

[31] Yu Wai Man CY, Chinnery PF, Griffiths PG. Extraocular muscles have fundamentally distinct properties that make them selectively vulnerable to certain disorders. Neuromuscul Disord 2005;15(1):17–23. doi:10.1016/j.nmd.2004.10.002.

[32] Rocha MC, Grady JP, Grünewald A, Vincent A, Dobson PF, Taylor RW, et al. A novel immunofluorescent assay to investigate oxidative phosphorylation deficiency in mitochondrial myopathy: understanding mechanisms and improving diagnosis. Sci Rep 2015;5:1–17. doi:10.1038/srep15037.